

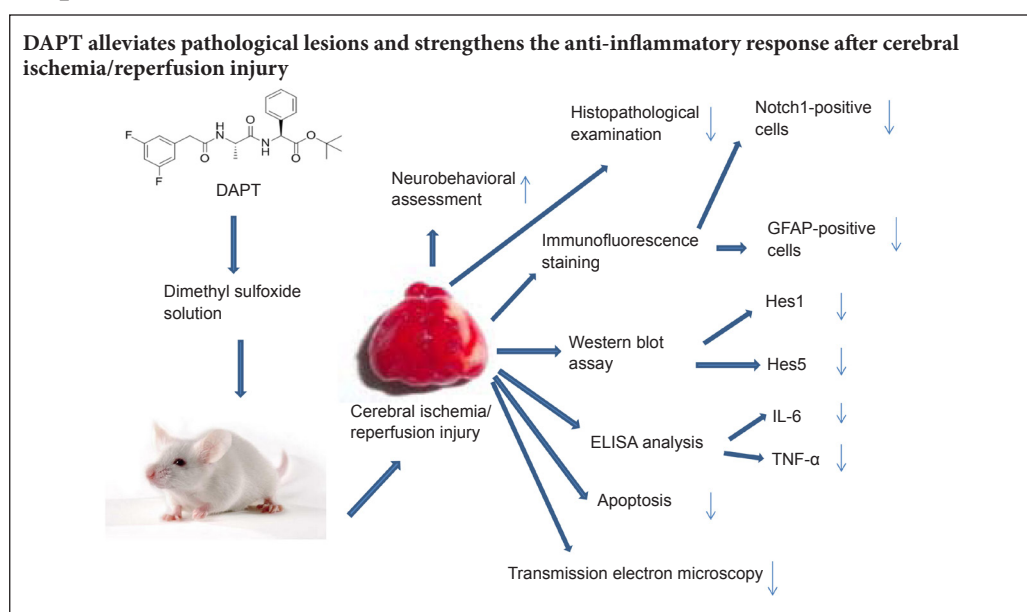
# Neuroprotective effect of Notch pathway inhibitor DAPT against focal cerebral ischemia/reperfusion 3 hours before model establishment

Jun-Jie Wang, Jun-De Zhu\*, Xian-Hu Zhang, Ting-Ting Long, Guo Ge, Yan Yu

Department of Anatomy, School of Basic Medicine, Guizhou Medical University, Gui'an New District, Guizhou Province, China

**Funding:** This study was supported by the National Natural Science Foundation of China, No. 81660243 (to JDZ); a grant from the Social Development Science and Technology Plan Project of Science and Technology Department of Guizhou Province of China, No. SY [2015] 3041 (to JDZ); a grant from the Science and Technology Department of Guizhou Province of China, No. LG [2012] 028 (to JDZ).

## Graphical Abstract



\*Correspondence to:

Jun-De Zhu, MS,  
jdzhu73@126.com.

orcid:

0000-0001-9666-8010  
(Jun-De Zhu)

doi: 10.4103/1673-5374.245469

Received: May 28, 2018

Accepted: August 15, 2018

## Abstract

As an inhibitor of the Notch signaling pathway, N-[N-(3,5-difluorohenacetyl)-l-alanyl]-S-phenylglycine tert-butyl ester (DAPT) may protect brain tissue from serious ischemic injury. This study aimed to explore neuroprotection by DAPT after cerebral ischemia/reperfusion (I/R) injury. DAPT was intraperitoneally injected 3 hours before the establishment of a focal cerebral I/R model in the right middle cerebral artery of obstructed mice. Longa scores were used to assess neurological changes of mice. Nissl staining and TdT-mediated dUTP-biotin nick-end labeling staining were used to examine neuronal damage and cell apoptosis in the right prefrontal cortex, while immunofluorescence staining was used to detect glial fibrillary acidic protein- and Notch1-positive cells. Protein expression levels of Hes1 and Hes5 were detected by western blot assay in the right prefrontal cortex. Our results demonstrated that DAPT significantly improved neurobehavioral scores and relieved neuronal morphological damage. DAPT decreased the number of glial fibrillary acidic protein- and Notch1-positive cells in the right prefrontal cortex, while also reducing the number of apoptotic cells and decreasing interleukin-6 and tumor necrosis factor- $\alpha$  contents, and simultaneously downregulating Hes1 and Hes5 protein expression. These findings verify that DAPT alleviates pathological lesions and strengthens the anti-inflammatory response after cerebral I/R injury. Thus, DAPT might be developed as an effective drug for the prevention of cerebral I/R injury.

**Key Words:** nerve regeneration; DAPT; cerebral ischemia; glial fibrillary acidic protein; Notch1; Hes1; Hes5; neural regeneration

**Chinese Library Classification No.** R453; R364; R741

## Introduction

Stroke is a major cause of death, adult chronic disability, and dementia. Ischemic stroke accounts for approximately 80% of stroke cases, which may be caused by hypertension, dyslipidemia, lifestyle, and/or genetic factors (Zhao et al., 2017). Many clinical methods, such as anticoagulation and thrombolysis treatment, have been used to treat cerebrovascular diseases; however, vascular recanalization could aggra-

vate brain tissue damage and cause delayed nerve cell death, thus eliciting cerebral ischemia/reperfusion (I/R) injury (Certo et al., 2015; Sadana et al., 2015; Hartig et al., 2017). Despite widespread research, there is no effective treatment for cerebral I/R injury so far. Therefore, understanding its molecular mechanisms may provide novel insights into the development of effective treatments for cerebral I/R injury.

The Notch pathway, an evolutionarily conserved signaling

system, has been recognized as an important adaptive signaling pathway that participates in various biological processes, such as neuronal proliferation, differentiation and apoptosis (Nemir and Pedrazzini, 2008; Wickremasinghe et al., 2011). Previous studies have shown that the classical biological effects of Notch signaling are mediated through interactions between Notch receptors and their ligands to release the Notch intracellular domain, which then forms a transcription-activating complex to regulate Notch-dependent gene expression, such as Hes1 and Hes5 (Mahler et al., 2010; Osathanon et al., 2013; Zhang et al., 2015). N-[N-(3,5-difluoroacetyl)-L-alanyl]-S-phenylglycine tert-butyl ester (DAPT), a common  $\gamma$ -secretase inhibitor, can effectively inhibit release of the Notch intracellular domain from the Notch receptor during the enzymatic digestion process (Lee et al., 2017).

Inflammatory responses and apoptosis are crucial mechanisms involved in cerebral I/R injury (Broughton et al., 2009; Siniscalchi et al., 2014). Recently, several studies found a significant reduction of blood flow in the ischemic core, whereby programmed cell apoptosis and inflammatory responses occurred in the ischemic penumbra (Xu and Zhang, 2011; Ghosh et al., 2012; Kalogeris et al., 2012; Hu et al., 2017). Moreover, DAPT could protect against renal I/R injury by suppressing inflammation and apoptosis (Huang et al., 2011). However, no direct evidence has indicated involvement of the Notch pathway in the protective effects of glial fibrillary acidic protein (GFAP) and/or Hes1 and Hes5 protein expression on cerebral I/R injury. Therefore, this study aimed to investigate the role of DAPT and its putative mechanism in mice with cerebral I/R injury to provide a new strategy for the prevention and treatment of cerebrovascular disease.

## Materials and Methods

### Animals

In total, 204 healthy male Kunming mice, aged 3–4 months and weighing 30–35 g, were purchased from the Experimental Animal Center of Guizhou Medical University, China [License No. SYXK(Qian) 2012-0004]. All mice were housed at 50–70% humidity and 22–24°C under a 12-hour light/dark cycle. All experiments were conducted in accordance with the guidelines of the Ministry of Health of China for Animal Care and Use. The study protocol was approved by the Experimental Animal Research Committee of Guizhou Medical University, China. Food and water were freely available during all phases of the experiment. Mice were randomly divided into a sham group ( $n = 68$ ), I/R group (I/R only) ( $n = 68$ ) and DAPT group (I/R + DAPT treatment) ( $n = 68$ ). Each group was divided into four subgroups: 1, 3, 7 and 14 days.

### Mouse models of focal cerebral ischemia/reperfusion injury

Mice were acclimated to the facility for one week prior to surgery. I/R mouse models were established as previously described by Longa et al. (1989). In brief, mice were intraperitoneally anesthetized with 5 mL/kg of 10% (w/v) chloral hydrate and secured on the operating table. Through a mid-line cervical incision, the bilateral common carotid arteries were exposed and gently separated from the carotid sheath

and vagus nerve. The right common carotid artery, internal carotid artery, and external carotid artery were exposed and isolated. A microvascular clamp (Roboz, Berlin, Germany) was used to temporarily clip the internal carotid artery. A small cut was made at the common carotid artery from the bifurcation 3–4 mm. A 2.0-cm nylon suture (diameter  $0.16 \pm 0.02$  mm) with its tip rounded by heating into the internal carotid artery was made until it closed the origin of the middle cerebral artery. Sham group mice underwent identical surgery, but did not have the suture inserted. The body temperature of mice was maintained at 37°C through all surgical and postoperative procedures until mice regained consciousness. After recovery from anesthesia, all mice were kept in the animal quarters with free access to food and water.

### Drug intervention

DAPT solution (20 mg/mL; MCE Co., Monmouth Junction, NJ) was prepared by dissolving DAPT powder in dimethyl sulfoxide. In the DAPT group, DAPT solution (5 mL/kg) was injected intraperitoneally 3 hours before middle cerebral artery occlusion. Mice in the other two groups were injected with 5 mL/kg dimethyl sulfoxide solution (Wang et al., 2015).

### Neurobehavioral assessment

According to the Longa scoring method (1989), neurobehavioral deficits were evaluated by an observer blinded to the identity of groups at 2 hours before sampling and rated on a scale of 0–4. Score 0: No obvious behavioral deficit. Score 1: Left forelimb showed a mild obvious neurobehavioral deficit and failed to straighten. Score 2: Mice showed a trend of circling to the left. Score 3: Mice spontaneously walked in a left circle. Score 4: Mice could not walk spontaneously and lost consciousness. Mice scored 1–3 were included in this study, but mice not showing behavioral deficits at the four time points were excluded from the study.

### Preparation of paraffin sections

In each subgroup, mice ( $n = 5$ ) were anesthetized with 5% (8 mL/kg) chloral hydrate and perfused with physiological saline via an aortic root catheter until the liver appeared to be white, followed by 4% paraformaldehyde solution that had been cooled to 4°C. Brains were removed and post-fixed in 4% paraformaldehyde solution overnight at 4°C. After dehydration and embedding in paraffin, 7- $\mu$ m coronal sections of brain were used for immunofluorescence, Nissl, and TdT-mediated dUTP-biotin nick-end labeling (TUNEL) staining.

### Nissl and TUNEL staining of the right prefrontal cortex

Paraffin sections were stained with Nissl (Solarbio Biotechnology, Beijing, China) and imaged using a light microscope (Olympus, Tokyo, Japan) at 400 $\times$  magnification. Apoptotic cells in brain sections were identified by the TUNEL staining kit (KeyGen BioTech, Nanjing, China) as previously described (Wicha et al., 2017). Paraffin sections were deparaffinized, treated with 3% hydrogen peroxide and TdT enzyme, and incubated with digoxigenin-conjugated antibodies. Sections were photographed using a light microscope (Olympus). Nissl- and TUNEL-positive cells were counted using Image-Pro Plus 6.0

software (Media Cybernetics, Silver Spring, MD, USA).

### Immunofluorescence staining

To detect Notch1- and GFAP-positive cells in the right cerebral cortex of the ischemic hemisphere, brain sections were incubated for 30 minutes in 2.0 M HCl to denature DNA, and the reaction was neutralized in 0.1 M boric acid for 10 minutes. Thereafter, brain sections were rinsed in phosphate-buffered saline (PBS) containing 0.3% Triton for 30 minutes, preincubated in 10% normal goat serum for 2 hours at room temperature, and incubated with polyclonal rabbit anti-Notch1 (1:150; Biosynthesis Biotechnology, Beijing, China) and monoclonal rabbit anti-GFAP (astrocyte marker) antibody (1:200; Boster Biotechnology, Wuhan, China) at 4°C overnight, and then incubated with Cy3-conjugated affinity-purified goat anti-rabbit IgG (1:100; Sigma, St. Louis, MO, USA) in a humidified chamber for 1 hour at 37°C. Anti-Notch1 and anti-GFAP were used as cell-type specific markers in each brain section. Numbers of Notch1- and GFAP-positive cells were counted by laser-scanning confocal microscopy (Olympus).

### Western blot assay

Mice ( $n = 5$ ) from each subgroup were anesthetized with 5% (8 mL/kg) chloral hydrate, and perfused with physiological saline rapidly *via* an aortic root catheter. Brains were removed quickly and frozen at  $-80^{\circ}\text{C}$ . Brain tissue from the right cerebral cortex was homogenized by adding protein extraction buffer at a 1:5 volume to tissue weight in a glass homogenizer. Sample protein concentrations were determined using a bicinchoninic acid assay kit (Beyotime Biotechnology, Shanghai, China). Hes1 and Hes5 proteins were loaded onto 5% stacking/10% separating sodium dodecyl sulphate-polyacrylamide gels (Solarbio Biotechnology, Beijing, China) for electrophoresis, and then transferred onto polyvinylidene difluoride membranes (Millipore, Billerica, MA, USA). After blocking with 5% skimmed milk powder, membranes were incubated with rabbit polyclonal anti-Hes1, anti-Hes5 (1:200; Biosynthesis Biotechnology), and rabbit polyclonal anti- $\beta$ -actin (1:4000; ImmunoWay, Plano, TX, USA) overnight at 4°C. After washing with PBS for approximately 15 minutes, membranes were incubated with horseradish peroxidase-conjugated secondary goat-anti-rabbit antibody (1:6000; Proteintech, Chicago, IL, USA) for 2 hours at room temperature. Proteins were visualized using a sensitivity-enhanced chemiluminescence solution (Millipore). Finally, the intensity of blots was quantified using a Multi-Functional Imaging System (Bio-Rad, Hercules, CA, USA). Relative amounts of proteins were calculated as the ratio of Hes1 or Hes5 to  $\beta$ -actin.

### Transmission electron microscopy

Transmission electron microscopy was used to evaluate neuronal ultrastructural changes within the right prefrontal cortex in each subgroup ( $n = 2$ ). Brain tissues from the right prefrontal cortex were cut into  $1\text{ mm}^3$  sections and immediately fixed in 2.5% glutaraldehyde solution at 4°C overnight. After washing with 0.1 M PBS (pH 7.4), sections were fixed with 1% osmic acid (Pelco, CA, USA) for approximately 1

hour. Following dehydration in ethyl alcohol, brain tissues were embedded in Epon-Araldite resin (EMS, San Francisco, CA, USA), cut into ultrathin sections (approximately 50 nm), examined with transmission electron microscopy (Hitachi-7500, Tokyo, Japan), and imaged.

### Enzyme-linked immunosorbent assay

Remnant mice from each group were sacrificed at different time points. The right prefrontal cortex was separated and cleared by cold saline to prepare 10% fresh brain tissue homogenates. According to the manufacturer's protocol (Neo Bioscience, Beijing, China), amounts of interleukin-6 (IL-6) and tumor necrosis factor- $\alpha$  (TNF- $\alpha$ ) released in the right prefrontal cortex were measured by enzyme-linked immunosorbent assay.

### Statistical analysis

Data are expressed as the mean  $\pm$  standard deviation (SD). All data were analyzed using SPSS 19.0 software (SPSS, Chicago, IL, USA) by an observer blinded to experimental groupings. A one-way analysis of variance followed by Student-Newman-Keuls test was used to assess statistical significance. A value of  $P < 0.05$  was considered statistically significant.

## Results

### DAPT improves neurobehavioral deficits of cerebral I/R mice

The results of neurobehavioral scores are shown in **Figure 1**. In the sham group, there was no obvious neurologic dysfunction in mice. Cerebral I/R mice showed more severe neurological function injury compared with the sham group ( $P < 0.01$ ). After DAPT treatment, neurobehavioral deficits were significantly improved ( $P < 0.05$ ).

### DAPT alleviates pathological injury of neurons

The sham group showed normal neural structures with clear cell outlines, central nuclei, and abundant Nissl bodies in the cytoplasm (**Figure 2A and B**). In contrast, neural cells of the I/R group showed obvious injury, with shrunken cell bodies, pyknosis, and breaking and dissolution of nuclei. In the 1-day

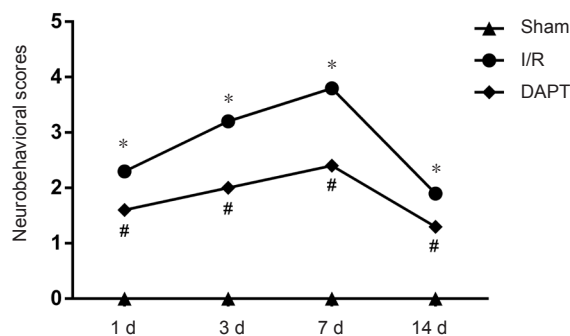


**Figure 1** Neurobehavioral scores of cerebral I/R mice following DAPT treatment.

Zea-Longa's neurobehavioral score was obtained for each group. Higher scores represent more severe neurological function deficits. Data are shown as the mean  $\pm$  SD ( $n = 20$  per subgroup; one-way analysis of variance followed by Student-Newman-Keuls test). \* $P < 0.01$ , vs. sham group; # $P < 0.05$ , vs. I/R group. I/R: Ischemia/reperfusion; DAPT: N-[N-(3,5-difluorohenacetyl)-l-alanyl]-S-phenylglycine tert-butyl ester; d: day(s).

I/R subgroup, neurons presented slight injury. In the 3-day I/R subgroup, neurons were disorganized and nuclear pyknosis occurred. Neurons exhibited the worst damage (Nissl bodies dissolved or disappeared) in the 7-day I/R subgroup. Cellular kernel pyknosis displayed as triangular-shaped cells. The clearance surrounding between neural cells was widened (Figure 2D). Numbers of neurons in the 14-day I/R subgroup increased and the damage was slightly relieved compared with the 7-day I/R subgroup. However, compared with the I/R subgroup, DAPT could alleviate neuronal damage in the DAPT group at different time points (Figure 2I and K).

#### DAPT decreases cell apoptosis

In the sham group, no obvious TUNEL-positive cells were observed in the right prefrontal cortex of brain tissues (Figure 3). Compared with the sham group, a few TUNEL-positive cells appeared in cerebral I/R mice ( $P < 0.01$ ; Figure 3J). Quantitative analyses (Figure 3J) demonstrated significantly less TUNEL-positive neurons in the DAPT group than in the I/R group ( $P < 0.05$ ).

#### DAPT decreases GFAP-positive cells

In the sham group, a few GFAP-positive cells appeared (Figure 4A). In the 1-day I/R subgroup, GFAP-positive cells began to increase compared with the sham group (Figure 4B). In the 3-day I/R subgroup, GFAP-positive cells exhibited star shapes and were also significantly enhanced compared with the sham group, but GFAP-positive cells were significantly decreased in the DAPT group ( $P < 0.01$ ) (Figure 4C and J). In addition, among the four subgroups of the I/R group, GFAP-positive cells reached a peak at 7 days, and showed thickened and shortened processes (Figure 4D). Compared with the 14-day I/R subgroup, numbers of GFAP-positive cells decreased and cell staining became shallower in the DAPT group ( $P < 0.01$ ; Figure 4E and J). These results indicated that cerebral I/R injury increased the expression of GFAP-positive cells and induced activation of gliosis. However, DAPT treatment evidently suppressed the activation of astrocytes with small cell bodies and slender processes at four time points (Figure 4F-J).

#### DAPT reduces Notch1-positive cells

Notch1-positive signal was concentrated in the cytoplasm, while nuclei were dyed blue by 4',6-diamidino-2-phenylindole (DAPI). As shown in Figure 5A, a few Notch1-positive cells were observed in the sham group. Compared with the sham group, more Notch1-positive cells appeared in the cerebral cortex of the I/R group at each time point ( $P < 0.01$ ; Figure 5B-J). After DAPT treatment, Notch1-positive cells were decreased compared with the I/R group at different time points ( $P < 0.05$ ; Figure 5F-J). Among the four DAPT treatment subgroups, numbers of Notch1-positive cells remained highest at 7 days.

#### DAPT inhibits expression of Hes1 and Hes5

Hes1 and Hes5 protein expression levels in the right prefrontal cortex were measured by western blot assay, as

shown in Figure 6. Compared with the sham group, protein expression of Hes1 and Hes5 was increased in the I/R group ( $P < 0.01$ ). However, the two proteins were remarkably decreased in the DAPT group compared with the I/R group at different time points ( $P < 0.05$ ).

#### DAPT alleviates ultrastructural damage of neurons

In the sham group, neurons exhibited abundant organelles in the cytoplasm (Figure 7A). However, neurons in the prefrontal cortex of the I/R group showed varying degrees of damage at different time points (Figure 7B-E). In the 1-day I/R subgroup, organelles were disordered, intracellular spaces became large, and the mitochondria swelled slightly (Figure 7B). In the 3-day I/R subgroup, nuclei became pyknotic and mitochondria were markedly swelled (Figure 7C). In the 7-day I/R subgroup, neuronal ultrastructural damage was most severe with incomplete nuclear envelopes and dissolved organelles (Figure 7D). In the 14-day I/R subgroup, the cristae of some mitochondria were fractured and the number of organelles was increased compared with the 7-day subgroup (Figure 7E). Results shown in Figure 7F-I revealed that DAPT treatment alleviated neuronal ultrastructural damage in mice after middle cerebral artery occlusion.

#### DAPT inhibits production of IL-6 and TNF- $\alpha$

As shown in Figure 8, compared with the sham group, IL-6 and TNF- $\alpha$  contents were significantly increased in each I/R subgroup ( $P < 0.01$ ). Indeed, contents of IL-6 and TNF- $\alpha$  in the I/R group became gradually elevated within the first 7 days and decreased from 7 to 14 days. However, IL-6 and TNF- $\alpha$  contents were significantly inhibited following DAPT treatment ( $P < 0.05$ ).

## Discussion

Stroke is a common cerebrovascular disorder in the aging population and constitutes the second highest principle cause of mortality (Guan et al., 2017). Ischemic stroke involves a complex pathophysiological process, appearing as calcium overload, inflammatory response, oxidative stress, and brain edema (Lee et al., 2017; Tamaki et al., 2017). Despite use of effective endovascular therapy, clinical outcomes after acute cerebral ischemic stroke remain poor (Goyal et al., 2016). As the result of severe neurological complications caused by stroke, neuroprotection in this disorder has recently become an increasingly hot topic (Zhu et al., 2012). Studies have found that the infarct area is formed by long-term ischemia, which is first focused within the ischemic center and then involves surrounding tissue, leading to an ischemic penumbra (Huang et al., 2015; Zhu et al., 2017). Restoring the perfusion of ischemic penumbra is a common clinical treatment to maintain the structural and functional integrity of neurons by inhibiting the inflammatory response (Heiss et al., 1997; Song and Yu, 2014; Liu et al., 2017).

Many studies have shown that middle cerebral artery infarction has become the main cause of ischemia in the clinic (Wijdicks et al., 2014; Chen et al., 2018). The focal cerebral ischemia model of middle cerebral artery occlusion could

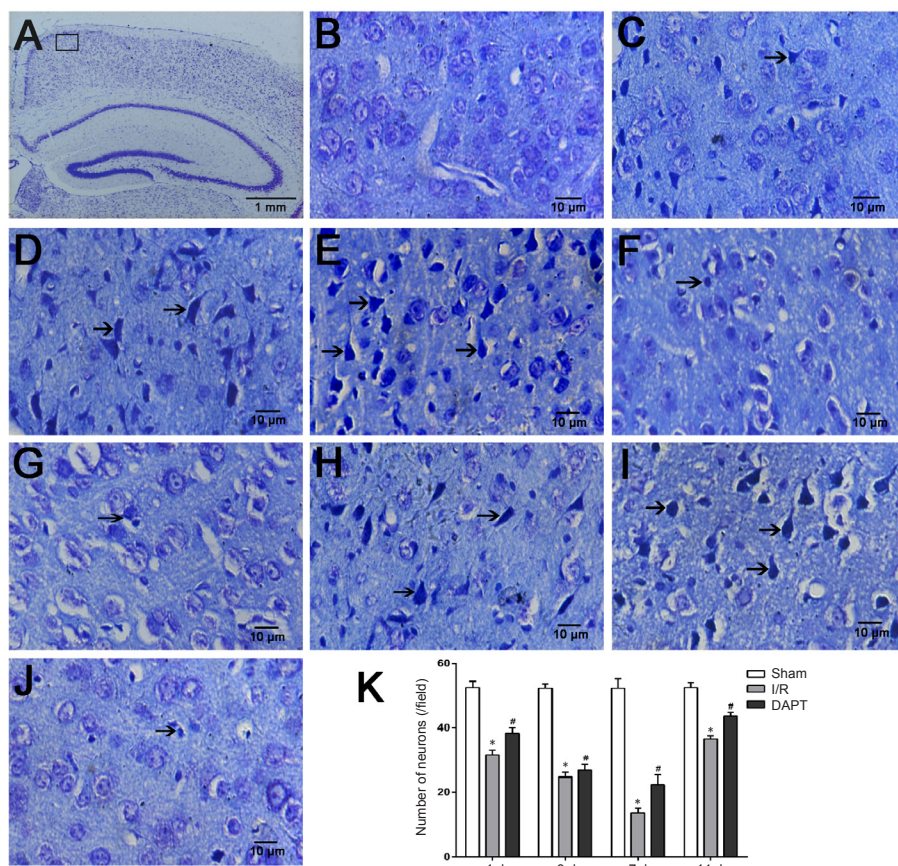


**Figure 2** Neurons of the right prefrontal cortex in cerebral I/R mice following DAPT treatment as assessed by optical microscopy.

(A) Right cerebral cortex area of mice: box indicates right prefrontal cortex. Scale bar: 1 mm. (B–J) Magnified figures of the box from A (Scale bars: 10  $\mu$ m). (B) Sham group: Neurons were arranged normally, and Nissl bodies in the cytoplasm were abundant. (C) 1-day I/R subgroup; (D) 3-day I/R subgroup; (E) 7-day I/R subgroup; (F) 14-day I/R subgroup; (G) 1-day DAPT subgroup; (H) 3-day DAPT subgroup; (I) 7-day DAPT subgroup; (J) 14-day DAPT subgroup; (K) Quantitation of Nissl-positive cells at 400 $\times$  magnification. Data are shown as the mean  $\pm$  SD ( $n = 5$  per subgroup; one-way analysis of variance followed by Student-Newman-Keuls test). \* $P < 0.01$ , vs. sham group; # $P < 0.05$ , vs. I/R group. I/R: Ischemia/reperfusion; DAPT: N-[N-(3,5-difluorohenacetyl)-l-alanyl]-S-phenylglycine tert-butyl ester; d: day(s).

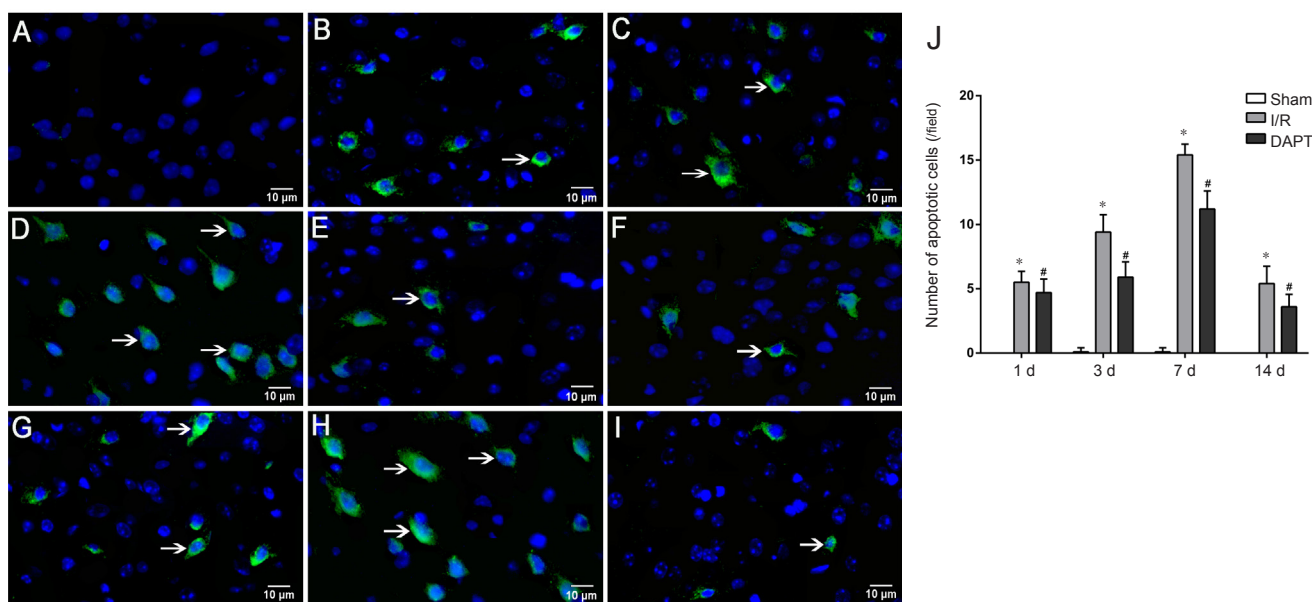


**Figure 3** Cell apoptosis in the right prefrontal cortex area in cerebral I/R mice following DAPT treatment, as assessed by fluorescence microscopy.

(A–I) Representative images of TUNEL staining at 400 $\times$  magnification. Apoptotic cells were labeled green, while nuclei were labeled blue with DAPI in A–I. Scale bars: 10  $\mu$ m. (A) Sham group: No obvious apoptotic cells. (B–E) 1-day, 3-day, 7-day, and 14-day I/R subgroups, respectively: numbers of apoptotic cells was increased compared with the sham group (arrows). (F–I) 1-day, 3-day, 7-day, and 14-day DAPT subgroups, respectively: numbers of apoptotic cells was reduced compared with the I/R group (arrows). (J) Number of apoptotic cells (number/view). Data are expressed as the mean  $\pm$  SD ( $n = 5$  per group at each time point; one-way analysis of variance followed by Student-Newman-Keuls test). \* $P < 0.01$ , vs. sham group; # $P < 0.05$ , vs. I/R group. I/R: Ischemia/reperfusion; TUNEL: TdT-mediated dUTP-biotin nick-end labeling; DAPT: N-[N-(3,5-difluorohenacetyl)-l-alanyl]-S-phenylglycine tert-butyl ester; DAPI: 4',6-diamidino-2-phenylindole; d: day(s).

simulate pathological processes of ischemic cerebrovascular disease and cause mice to show symptoms similar to humans. Previous studies demonstrated a strong association between the hippocampus and prefrontal cortex and age-related cognitive decline (Paulesu et al., 1993; Levy and Goldman-Rakic, 1999). Ischemic stroke is a serious disease and threat to the cognitive abilities of people. Thus, in our present study, the right prefrontal cortex was chosen to investigate the function of neural cells.

Nissl staining is a commonly used histological method to access morphological changes of cells (Shen et al., 2014). From the results of our light microscopy and transmission electron microscopy, neural structure was normal in the sham group, with abundant organelles exhibiting clear structures. In the I/R group, the distribution and arrangement of neural cells was irregular and mitochondria presented swelling, vacuolization, and even dissolution. Apoptosis is one of the major pathogenic mechanisms underlying cerebral I/R injury (Broughton et al., 2009). Blocking neuronal apoptosis could prevent the loss of neuronal cells, minimize brain injury induced by I/R damage, and slow the onset of cerebral ischemia and necrosis (Xie et al., 2011). In the present study, I/R surgery induced increases of TUNEL-positive cells in the right prefrontal cortex. Consistent with previous studies, cerebral I/R injury could cause severe brain damage, increased apoptosis, and destroy normal structure (Deng et al., 2015; Tang et al., 2017).

Proinflammatory cytokines, such as TNF- $\alpha$ , IL-6 and IL-1 $\alpha$ , have emerged as significant contributors to myocardial and cerebrovascular dysfunction (Sun et al., 2012; Kraft et al., 2017). Among several inflammatory factors, TNF- $\alpha$  appears to be the major pro-inflammatory cytokine with multiple mechanisms that promote inflammatory reactions (Di Paola et al., 2013). IL-6, which is produced by monocytes, macrophages and endothelial cells, is a multi-functional single chain glycoprotein cytokine with broad biological activity (Aloisi et al., 1992; Choi et al., 2017). It exhibits a rapid increase during the early stage of cerebral I/R injury, along with TNF- $\alpha$  and IL-1 $\beta$  (Frangogiannis, 2007; Wong and Crack, 2008). In this study, IL-6 and TNF- $\alpha$  expression in the I/R group increased significantly, in line with the results of previous studies (Baskaya et al., 2000; Shichita et al., 2012; Sanderson et al., 2013). Furthermore, when cerebral I/R injury occurred, release of IL-1 $\beta$ , TNF- $\alpha$ , IL-6 and other inflammatory factors increased the inflammation reaction, leading to irreversible neuronal damage and even apoptosis or necrosis (Siniscalchi et al., 2014).

The Notch pathway is known to regulate homeostasis and development in diverse organs, such as lung (Xu et al., 2012), liver (Kobayashi et al., 2002; Zhang et al., 2017), kidney (Barak et al., 2012) and heart (Yu et al., 2015; Luxan et al., 2016). Moreover, the Notch pathway plays a vital role in immune homeostasis, which exploits the ability to mediate intercellular communication (Nistri et al., 2017). In mammalian cells, four distinct Notch receptors (Notch1–4) and five Notch ligands have been identified (Guruharsha et al., 2012; Zhang et al., 2015; Lu et al., 2018). DAPT, a  $\gamma$ -secretase inhibitor, is

regarded as a Notch signaling pathway inhibitor (Cao et al., 2015). In recent years, DAPT has been widely used in the study of Alzheimer's disease, atherosclerosis, and neuroblastoma (Espinoza and Miele, 2013; Qin et al., 2016). DAPT could inhibit IL-6 secretion and restrain the activation of inflammatory responses during rheumatoid arthritis (Jiao et al., 2012). Similarly, Arumugam et al. (2006) reported that DAPT could reduce neuronal damage in the focal ischemic stroke model by restraining activation of microglial cells.

Hes1 and Hes5 are important downstream target genes in the Notch signaling pathway. Indeed, expression of Hes1 and Hes5 correlates with expression of Notch1, an important component of Notch signaling. Expression levels of Notch1, Hes1, and Hes5 respond well to regulation of the Notch signaling pathway (Yoon and Gaiano, 2005; Du et al., 2013). In our study, we demonstrated that DAPT was an effective inhibitor that could markedly depress expression of Notch1, Hes1, and Hes5. By Nissl staining and transmission electron microscopy, DAPT treatment could increase the number of intact neurons, and extenuate cellular edema and mitochondrial swelling. In the DAPT group, numbers of apoptotic cells and contents of IL-6 and TNF- $\alpha$  were obviously reduced. Accordingly, DAPT may have a positive effect on protecting brain tissue by inhibiting the inflammatory response and decreasing apoptosis.

Astrocytes are the most abundant glial cells in the brain and GFAP is considered one of the major marker proteins in mature astrocytes (Gomes et al., 1999; Middeldorp and Hol, 2011). In addition, astrocytes play a vital role in providing general structural, metabolic, and trophic support to neurons in brain tissue (Kamphuis et al., 2012). It was found that when stroke occurred, astrocytes proliferated and became activated; that is, the cell soma enlarged and processes became shortened and thickened (Hol and Pekny, 2015; Minhas et al., 2017). Astrocytes could promote the recovery of nerve function by isolating the infarct, reconstructing the blood-brain barrier, and repairing damaged neurons (Kimmelberg and Nedergaard, 2010; Sofroniew and Vinters, 2010). In addition, GFAP expression was suppressed by DAPT treatment in neonatal rats following hypoxic-ischemic brain injury (Xu and Zhang, 2011). Hence, increasing evidence suggests an important role of astrocytes in the nervous system. Our results showed that compared with the I/R group, expression of GFAP decreased after DAPT treatment. DAPT could inhibit gliosis and further improve cerebral ischemia.

In conclusion, DAPT ameliorates neuronal structural damage of the right prefrontal cortex and improves neural function. DAPT may activate mechanisms of anti-inflammation and anti-apoptosis by inhibiting the expression of GFAP. Our findings offer further theoretical evidence for DAPT as a potential therapeutic drug for cerebral I/R injury. However, the effects of DAPT on other mechanisms of cerebral I/R injury, such as reactive oxygen species and leukocyte infiltration, still require further investigation in our future studies.

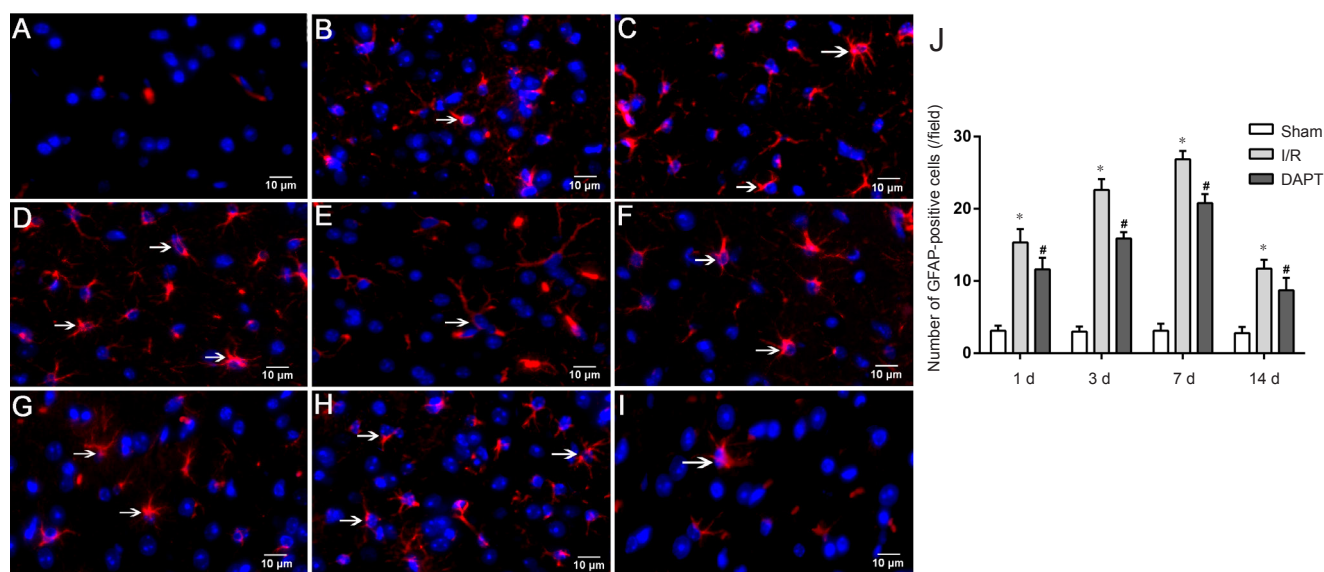


**Figure 4 Immunofluorescence microscopy of GFAP in the right prefrontal cortex of cerebral I/R mice following DAPT treatment.** (A–I) GFAP-immunoreactive cells (arrows) were examined in the prefrontal cortex by immunofluorescence labeling at 400× magnification. GFAP-positive cells were labeled red, and the labeling was mainly localized to the cytoplasm. Nuclei were labeled blue with DAPI in A–I. Scale bars: 10 μm. (A) Sham group: A few GFAP-immunoreactive cells. (B–E) 1-day, 3-day, 7-day, and 14-day I/R subgroups, respectively: More GFAP-positive cells were visible compared with the sham group (arrows). (F–I) 1-day, 3-day, 7-day, and 14-day DAPT subgroups, respectively: fewer GFAP-positive cells were observed compared with the I/R group (arrows). (J) Quantitation analysis of GFAP-immunoreactive cells. Data are expressed as the mean ± SD ( $n = 5$  per subgroup; one-way analysis of variance followed by Student-Newman-Keuls test). \* $P < 0.01$ , vs. sham group; # $P < 0.05$ , vs. I/R group. I/R: Ischemia/reperfusion; DAPT: N-[N-(3,5-difluorobenzenyl)-l-alanyl]-S-phenylglycine tert-butyl ester; GFAP: glial fibrillary acidic protein; DAPI: 4',6-diamidino-2-phenylindole; d: day(s).

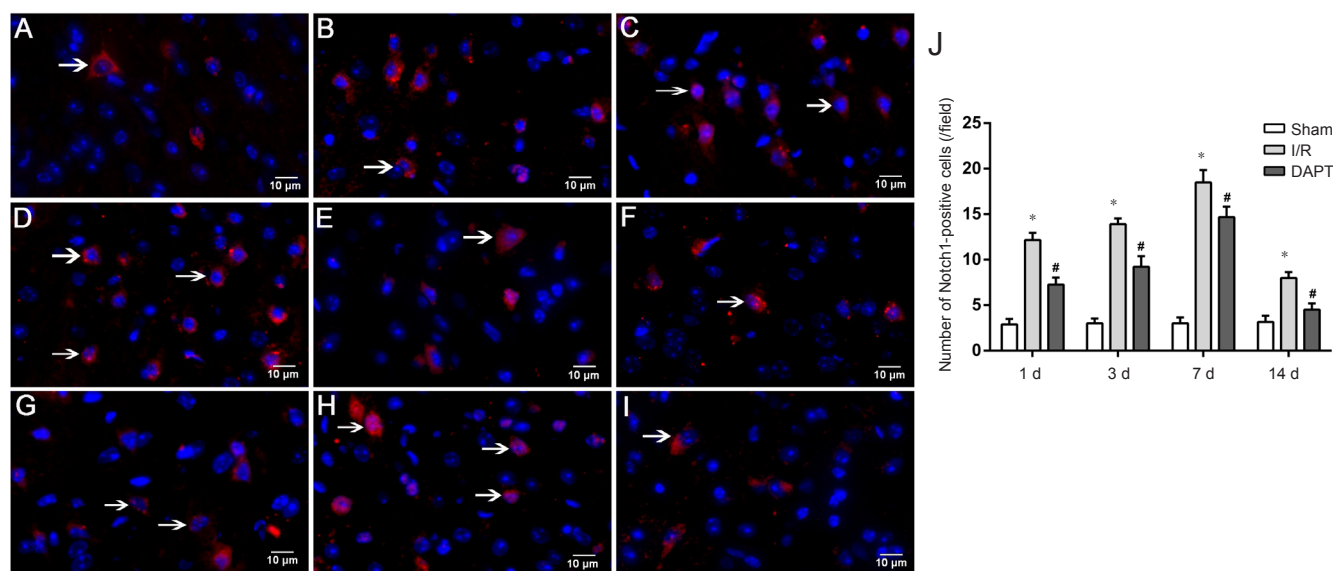


**Figure 5 Immunofluorescence microscopy of Notch1 in the prefrontal cortex area of cerebral I/R mice following DAPT treatment.** (A–I) Notch1-immunoreactive cells were examined in the prefrontal cortex by immunofluorescence labeling at 400× magnification. Scale bars: 10 μm. (A) Sham group: A few Notch1-immunoreactive cells. (B–E) 1-day, 3-day, 7-day, and 14-day I/R subgroups, respectively: more Notch1-positive cells were detectable compared with the sham group (arrows). (F–I) 1-day, 3-day, 7-day, and 14-day DAPT subgroups, respectively: fewer Notch1-positive cells were apparent compared with the I/R group (arrows). (J) Quantification of Notch1-positive cells. Data are expressed as the mean ± SD ( $n = 5$  per group at each time point; one-way analysis of variance followed by Student-Newman-Keuls test). \* $P < 0.01$ , vs. sham group; # $P < 0.05$ , vs. I/R group. I/R: Ischemia/reperfusion; DAPT: N-[N-(3,5-difluorobenzenyl)-l-alanyl]-S-phenylglycine tert-butyl ester; d: day(s).

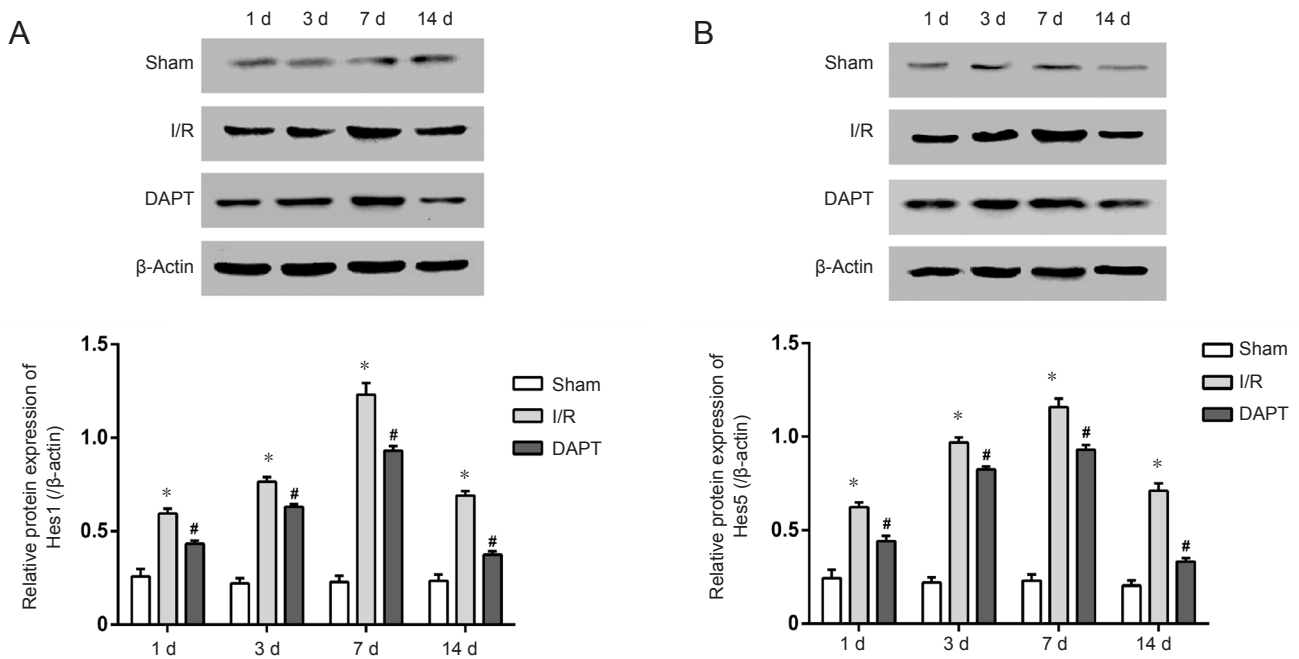


**Figure 6** Western blot assay for Hes1 (A) and Hes5 (B) protein expression in the right prefrontal cortex of cerebral I/R mice following DAPT treatment.

Expression was calculated as the ratio of optical density of the target protein to that of  $\beta$ -actin. Data are expressed as the mean  $\pm$  SD ( $n = 5$  per group at each time point; one-way analysis of variance followed by Student-Newman-Keuls test). \* $P < 0.01$ , vs. sham group; # $P < 0.05$ , vs. I/R group. I/R: Ischemia/reperfusion; DAPT: N-[N-(3,5-difluorobenzenyl)-L-alanyl]-S-phenylglycine tert-butyl ester; d: day(s).

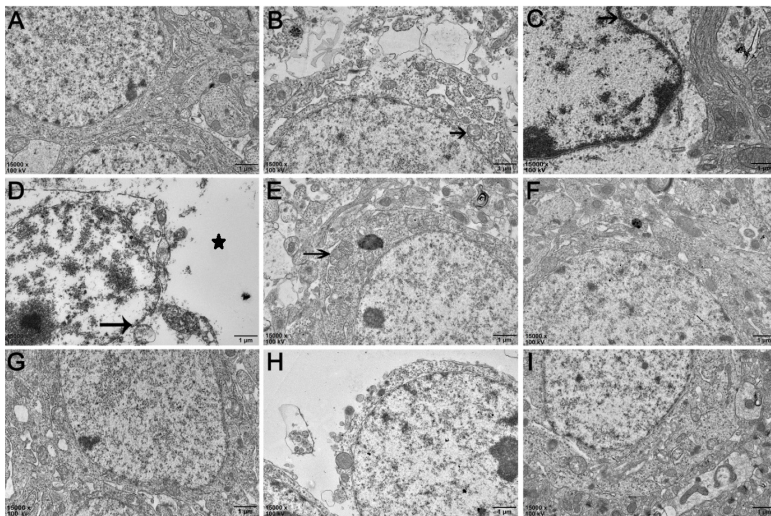


**Figure 7** Ultrastructure of neurons of the right prefrontal cortex in cerebral I/R mice following DAPT treatment under a transmission electron microscope.

(A) Sham group: Neurons exhibited abundant organelles; (B) 1-day I/R subgroup: organelles were disordered and mitochondria swelled slightly (arrow); (C) 3-day I/R subgroup: nucleus exhibited pyknosis (arrow); (D) 7-day I/R subgroup: neuron exhibited incomplete nuclear envelope (arrow) and dissolved organelles (star); (E) 14-day I/R subgroup: cristae of some mitochondria were fractured (arrow); (F) 1-day DAPT subgroup; (G) 3-day DAPT subgroup; (H) 7-day DAPT subgroup; (I) 14-day DAPT subgroup. Scale bars: 1.0  $\mu$ m. I/R: Ischemia/reperfusion; DAPT: N-[N-(3,5-difluorobenzenyl)-L-alanyl]-S-phenylglycine tert-butyl ester.

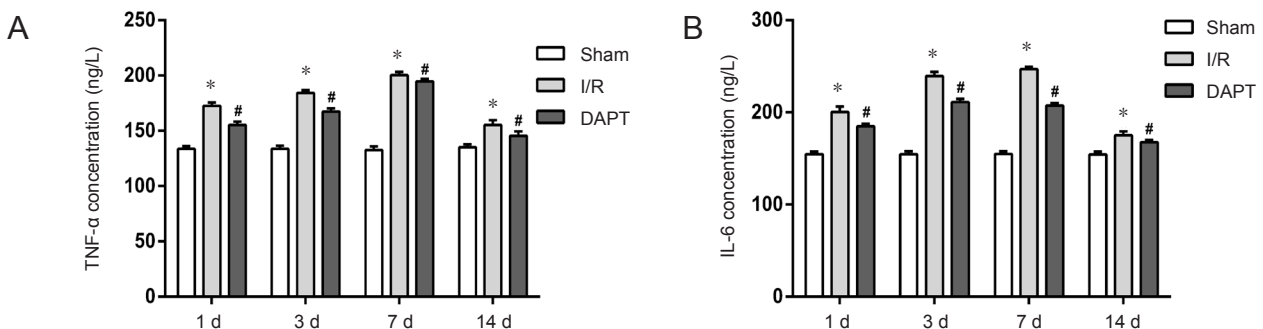


**Figure 8** Contents of TNF- $\alpha$  (A) and IL-6 (B) in the prefrontal cortex in cerebral I/R mice following DAPT treatment (enzyme linked immunosorbent assay).

Data are presented as the mean  $\pm$  SD ( $n = 5$ ; one-way analysis of variance followed by Student-Newman-Keuls test). \* $P < 0.01$ , vs. sham group; # $P < 0.05$ , vs. I/R group. d: Day(s).

**Author contributions:** Concept and design of the study: JJW and JDZ; experiment implementation: JDZ, JJW, XHZ, YY, and TTL; data analysis: GG; provided reagents/materials/analysis tools: JJW and XHZ; paper writing: JJW. All authors approved the final version of the paper.

**Conflicts of interest:** The authors declare that no conflict of interest exists.

**Financial support:** This study was supported by the National Natural Science Foundation of China, No. 81660243 (to JDZ); a grant from the Social Development Science and Technology Plan Project of Science and Technology Department of Guizhou Province of China, No. SY [2015] 3041 (to JDZ); a grant from the Science and Technology Department of Guizhou Province of China, No. LG [2012] 028 (to JDZ). The funders did not participate in data collection and analysis, article writing or submission.

**Institutional review board statement:** The study protocol was approved by the Experimental Animal Research Committee of Guizhou Medical University of China. The experimental procedure followed the National Institutes of Health Guide for the Care and Use of Laboratory Animals (NIH Publications No. 8023, revised 1985).

**Copyright license agreement:** The Copyright License Agreement has been signed by all authors before publication.

**Data sharing statement:** Datasets analyzed during the current study are available from the corresponding author on reasonable request.

**Plagiarism check:** Checked twice by iThenticate.

**Peer review:** Externally peer reviewed.

**Open access statement:** This is an open access journal, and articles are distributed under the terms of the Creative Commons Attribution-Non-Commercial-ShareAlike 4.0 License, which allows others to remix, tweak, and build upon the work non-commercially, as long as appropriate credit is given and the new creations are licensed under the identical terms.

**Open peer reviewer:** Maxime Gauberti, GIP Cyceron, Bd Henri Becquerel, France.

**Additional file:** Open peer review report 1.

## References

- Aloisi F, Care A, Borsellino G, Gallo P, Rosa S, Bassani A, Cabibbo A, Testa U, Levi G, Peschle C (1992) Production of hemolymphopoietic cytokines (IL-6, IL-8, colony-stimulating factors) by normal human astrocytes in response to IL-1 beta and tumor necrosis factor-alpha. *J Immunol* 149:2358-2366.
- Arumugam TV, Chan SL, Jo DG, Yilmaz G, Tang SC, Cheng A, Gleichmann M, Okun E, Dixit VD, Chigurupati S, Mughal MR, Ouyang X, Miele L, Magnus T, Poosala S, Granger DN, Mattson MP (2006) Gamma secretase-mediated Notch signaling worsens brain damage and functional outcome in ischemic stroke. *Nat Med* 12:621-623.
- Barak H, Surendran K, Boyle SC (2012) The role of Notch signaling in kidney development and disease. *Adv Exp Med Biol* 727:99-113.
- Baskaya MK, Dogan A, Rao AM, Dempsey RJ (2000) Neuroprotective effects of citicoline on brain edema and blood-brain barrier breakdown after traumatic brain injury. *J Neurosurg* 92:448-452.
- Broughton BR, Reutens DC, Sobey CG (2009) Apoptotic mechanisms after cerebral ischemia. *Stroke* 40:e331-e339.
- Cao Y, Cai J, Zhang S, Yuan N, Fang Y, Wang Z, Li X, Cao D, Xu F, Lin W, Song L, Wang Z, Wang J, Xu X, Zhang Y, Zhao W, Hu S, Zhang X, Wang J (2015) Autophagy sustains hematopoiesis through targeting Notch. *Stem Cells Dev* 24:2660-2673.
- Certo M, Endo Y, Ohta K, Sakurada S, Bagetta G, Amantea D (2015) Activation of RXR/PPARgamma underlies neuroprotection by bexarotene in ischemic stroke. *Pharmacol Res* 102:298-307.
- Chen DP, Hou SH, Guo Y, Hu ZZ, Hu XH, Chen YG, Chen MS (2018) Human placenta-derived mesenchymal stem cell transplantation provides neuroprotection against cerebral infarction in rats. *Zhongguo Zuzhi Gongcheng Yanjiu* 22:65-69.
- Choi HS, Hwang JK, Kim JG, Hwang HS, Lee SJ, Chang YK, Kim JI, Moon IS (2017) The optimal duration of ischemic preconditioning for renal ischemia-reperfusion injury in mice. *Ann Surg Treat Res* 93:209-216.
- Deng H, Zuo X, Zhang J, Liu X, Liu L, Xu Q, Wu Z, Ji A (2015) Alkali-protects against cerebral ischemia/reperfusion-induced injury in rats. *Mol Med Rep* 11:3659-3665.
- Di Paola R, Genovese T, Impellizzeri D, Ahmad A, Cuzzocrea S, Esposito E (2013) The renal injury and inflammation caused by ischemia-reperfusion are reduced by genetic inhibition of TNF-alphaR1: a comparison with infliximab treatment. *Eur J Pharmacol* 700:134-146.
- Du X, Li W, Gao X, West MB, Saltzman WM, Cheng CJ, Stewart C, Zheng J, Cheng W, Kopke RD (2013) Regeneration of mammalian cochlear and vestibular hair cells through Hes1/Hes5 modulation with siRNA. *Hearing Res* 304:91-110.
- Espinoza I, Miele L (2013) Notch inhibitors for cancer treatment. *Pharmacol Ther* 139:95-110.
- Frangogiannis NG (2007) Chemokines in ischemia and reperfusion. *Thromb Haemostasis* 97:738-747.
- Ghosh N, Yuan X, Turenus CI, Tone B, Ambadipudi K, Snyder EY, Obenaus A, Ashwal S (2012) Automated core-penumbra quantification in neonatal ischemic brain injury. *J Cereb Blood Flow Metab* 32:2161-2170.
- Gomes FC, Paulin D, Moura NV (1999) Glial fibrillary acidic protein (GFAP): modulation by growth factors and its implication in astrocyte differentiation. *Braz J Med Biol Res* 32:619-631.
- Goyal M, Menon BK, van Zwam WH, Dippel DW, Mitchell PJ, Demchuk AM, Dávalos A, Majoe CB, van der Lugt A, de Miquel MA, Donnan GA, Roos YB, Bonafé A, Jahan R, Diener HC, van den Berg LA, Levy EI, Berkhemer OA, Pereira VM, Rempel J, et al. (2016) Endovascular thrombectomy after large-vessel ischaemic stroke: a meta-analysis of individual patient data from five randomised trials. *Lancet* 387:1723-1731.
- Guan J, Wei X, Qu S, Lv T, Fu Q, Yuan Y (2017) Osthole prevents cerebral ischemia-reperfusion injury via the Notch signaling pathway. *Biochem Cell Biol* 95:459-467.
- Guruharsha KG, Kankel MW, Artavanis-Tsakonas S (2012) The Notch signalling system: recent insights into the complexity of a conserved pathway. *Nat Rev Genet* 13:654-666.
- Hartig W, Mages B, Aleithe S, Nitzsche B, Altmann S, Barthel H, Krueger M, Michalski D (2017) Damaged neocortical perineuronal nets due to experimental focal cerebral ischemia in mice, rats and sheep. *Front Integr Neurosci* 11:15.
- Heiss WD, Grond M, Thiel A, von Stockhausen HM, Rudolf J (1997) Ischaemic brain tissue salvaged from infarction with alteplase. *Lancet* 349:1599-1600.
- Hol EM, Pekny M (2015) Glial fibrillary acidic protein (GFAP) and the astrocyte intermediate filament system in diseases of the central nervous system. *Curr Opin Cell Biol* 32:121-130.
- Hu GQ, Du X, Li YJ, Gao XQ, Chen BQ, Yu L (2017) Inhibition of cerebral ischemia/reperfusion injury-induced apoptosis: nicotiflorin and JAK2/STAT3 pathway. *Neural Regen Res* 12:96-102.
- Huang H, Chen Y, Zhu F, Tang S, Xiao J, Li L, Lin X (2015) Down-regulated Na<sup>+</sup>/K<sup>+</sup>-ATPase activity in ischemic penumbra after focal cerebral ischemia/reperfusion in rats. *Int J Clin Exp Pathol* 8:12708-12717.
- Huang R, Zhou Q, Veeraragoo P, Yu H, Xiao Z (2011) Notch2/Hes-1 pathway plays an important role in renal ischemia and reperfusion injury-associated inflammation and apoptosis and the gamma-secretase inhibitor DAPT has a nephroprotective effect. *Ren Fail* 33:207-216.
- Jiao Z, Wang W, Ma J, Wang S, Su Z, Xu H (2012) Notch signaling mediates TNF-alpha-induced IL-6 production in cultured fibroblast-like synoviocytes from rheumatoid arthritis. *Clin Dev Immunol* 2012:350209.
- Kalogeris T, Baines CP, Krenz M, Korhuis RJ (2012) Cell biology of ischemia/reperfusion injury. *Int Rev Cell Mol Biol* 298:229-317.
- Kamphuis W, Mamber C, Moeton M, Kooijman L, Sluijs JA, Jansen AH, Vermeer M, de Groot LR, Smith VD, Rangarajan S, Rodriguez JJ, Orre M, Hol EM (2012) GFAP isoforms in adult mouse brain with a focus on neurogenic astrocytes and reactive astrogliosis in mouse models of Alzheimer disease. *PLoS One* 7:e42823.
- Kimelberg HK, Nedergaard M (2010) Functions of astrocytes and their potential as therapeutic targets. *Neurotherapeutics* 7:338-353.
- Kobayashi M, Takeyoshi I, Yoshinari D, Matsumoto K, Morishita Y (2002) p38 mitogen-activated protein kinase inhibition attenuates ischemia-reperfusion injury of the rat liver. *Surgery* 131:344-349.
- Kraft P, Scholtyschik K, Schuhmann MK, Kleinschnitz C (2017) Depletion of CD11c<sup>+</sup> cells does not influence outcomes in mice subjected to transient middle cerebral artery occlusion. *Neuroimmunomodulation* 24:123-131.
- Lee JC, Cho JH, Lee TK, Kim IH, Won MH, Cho GS, Shin BN, Hwang IK, Park JH, Ahn JH, Kang JJ, Lee YJ, Kim YH (2017) Effect of hyperthermia on calbindin-D 28k immunoreactivity in the hippocampal formation following transient global cerebral ischemia in gerbils. *Neural Regen Res* 12:1458-1464.

- Lee ML, Martinez-Lozada Z, Krizman EN, Robinson MB (2017) Brain endothelial cells induce astrocytic expression of the glutamate transporter GLT-1 by a Notch-dependent mechanism. *J Neurochem* 143:489-506.
- Levy R, Goldman-Rakic PS (1999) Association of storage and processing functions in the dorsolateral prefrontal cortex of the nonhuman primate. *J Neurosci* 19:5149-5158.
- Liu H, Zuo F, Wu H (2017) Blockage of cytosolic phospholipase A2 alpha by monoclonal antibody attenuates focal ischemic brain damage in mice. *Biosci Trends* 11:439-449.
- Lo EH, Dalkara T, Moskowitz MA (2003) Mechanisms, challenges and opportunities in stroke. *Nat Rev Neurosci* 4:399-415.
- Longa EZ, Weinstein PR, Carlson S, Cummins R (1989) Reversible middle cerebral artery occlusion without craniectomy in rats. *Stroke* 20:84-91.
- Lu L, Yue S, Jiang L, Li C, Zhu Q, Ke M, Lu H, Wang X, Busuttill RW, Ying QL, Kupiec-Weglinski JW, Ke B (2018) Myeloid Notch1 deficiency activates RhoA/ROCK pathway and aggravates hepatocellular damage in mouse ischemic livers. *Hepatology* 67:1041-1055.
- Luxan G, D'Amato G, MacGrogan D, de la Pompa JL (2016) Endocardial Notch signaling in cardiac development and disease. *Circ Res* 118:e1-18.
- Mahler J, Filippi A, Driever W (2010) DeltaA/DeltaD regulate multiple and temporally distinct phases of notch signaling during dopaminergic neurogenesis in zebrafish. *J Neurosci* 30:16621-16635.
- Middeldorp J, Hol EM (2011) GFAP in health and disease. *Prog Neurobiol* 93:421-443.
- Minhas G, Prabhakar S, Morishita R, Shimamura M, Bansal R, Anand A (2017) Transplantation of lineage-negative stem cells in pterygopalatine artery ligation induced retinal ischemia-reperfusion injury in mice. *Mol Cell Biochem* 429:123-136.
- Moskowitz MA, Lo EH, Iadecola C (2010) The science of stroke: mechanisms in search of treatments. *Neuron* 67:181-198.
- Nemir M, Pedrazzini T (2008) Functional role of Notch signaling in the developing and postnatal heart. *J Mol Cell Cardiol* 45:495-504.
- Nistri S, Sassoli C, Bani D (2017) Notch signaling in ischemic damage and fibrosis: evidence and clues from the heart. *Front Pharmacol* 8:187.
- Osathanon T, Manokawinchoke J, Nowwarote N, Aguilar P, Palaga T, Pavasant P (2013) Notch signaling is involved in neurogenic commitment of human periodontal ligament-derived mesenchymal stem cells. *Stem Cells Dev* 22:1220-1231.
- Paulesu E, Frith CD, Frackowiak RS (1993) The neural correlates of the verbal component of working memory. *Nature* 362:342-345.
- Qin WD, Zhang F, Qin XJ, Wang J, Meng X, Wang H, Guo HP, Wu QZ, Wu DW, Zhang MX (2016) Notch1 inhibition reduces low shear stress-induced plaque formation. *Int J Biochem Cell Biol* 72:63-72.
- Sadana P, Coughlin L, Burke J, Woods R, Mdzinarishvili A (2015) Anti-edema action of thyroid hormone in MCAO model of ischemic brain stroke: Possible association with AQP4 modulation. *J Neurol Sci* 354:37-45.
- Sanderson TH, Reynolds CA, Kumar R, Przyklenk K, Huttemann M (2013) Molecular mechanisms of ischemia-reperfusion injury in brain: pivotal role of the mitochondrial membrane potential in reactive oxygen species generation. *Mol Neurobiol* 47:9-23.
- Shen Y, Zhang A, Guo J, Dan G, Chen S, Yu H (2014) Fluorescence imaging of Evans blue extravasation into mouse brain induced by low frequency ultrasound with microbubble. *Biomed Mater Eng* 24:2831-2838.
- Shichita T, Hasegawa E, Kimura A, Morita R, Sakaguchi R, Takada I, Sekiya T, Ooboshi H, Kitazono T, Yanagawa T, Ishii T, Takahashi H, Mori S, Nishibori M, Kuroda K, Akira S, Miyake K, Yoshimura A (2012) Peroxiredoxin family proteins are key initiators of post-ischemic inflammation in the brain. *Nat Med* 18:911-917.
- Siniscalchi A, Gallelli L, Malferrari G, Pirritano D, Serra R, Santangelo E, De Sarro G (2014a) Cerebral stroke injury: the role of cytokines and brain inflammation. *J Basic Clin Physiol Pharmacol* 25:131-137.
- Sofroniew MV, Vinters HV (2010) Astrocytes: biology and pathology. *Acta Neuropathol* 119:7-35.
- Song M, Yu SP (2014) Ionic regulation of cell volume changes and cell death after ischemic stroke. *Transl Stroke Res* 5:17-27.
- Sun D, Huang J, Zhang Z, Gao H, Li J, Shen M, Cao F, Wang H (2012) Luteolin limits infarct size and improves cardiac function after myocardium ischemia/reperfusion injury in diabetic rats. *PLoS One* 7:e33491.
- Tamaki R, Orié SI, Alessandri B, Kempfski O, Heimann A (2017) Spreading depression and focal venous cerebral ischemia enhance cortical neurogenesis. *Neural Regen Res* 12:1278-1286.
- Tang Y, Tong X, Li Y, Jiang G, Yu M, Chen Y, Dong S (2017) JAK2/STAT3 pathway is involved in the protective effects of epidermal growth factor receptor activation against cerebral ischemia/reperfusion injury in rats. *Neurosci Lett* 662:219-226.
- Wang K, Zhang L, Rao W, Su N, Hui H, Wang L, Peng C, Tu Y, Zhang S, Fei Z (2015) Neuroprotective effects of crocin against traumatic brain injury in mice: Involvement of notch signaling pathway. *Neurosci Lett* 591:53-58.
- Wicha P, Tocharus J, Janyou A, Jittiwat J, Changtam C, Suksamrarn A, Tocharus C (2017) Hexahydrocurcumin protects against cerebral ischemia/reperfusion injury, attenuates inflammation, and improves antioxidant defenses in a rat stroke model. *PLoS One* 12:e189211.
- Wickremasinghe RG, Prentice AG, Steele AJ (2011) p53 and Notch signaling in chronic lymphocytic leukemia: clues to identifying novel therapeutic strategies. *Leukemia* 25:1400-1407.
- Wijdicks EF, Sheth KN, Carter BS, Greer DM, Kasner SE, Kimberly WT, Schwab S, Smith EE, Tamargo RJ, Wintermark M (2014) Recommendations for the management of cerebral and cerebellar infarction with swelling: a statement for healthcare professionals from the American Heart Association/American Stroke Association. *Stroke* 45:1222-1238.
- Wong CH, Crack PJ (2008) Modulation of neuro-inflammation and vascular response by oxidative stress following cerebral ischemia-reperfusion injury. *Curr Med Chem* 15:1-14.
- Xie M, Yi C, Luo X, Xu S, Yu Z, Tang Y, Zhu W, Du Y, Jia L, Zhang Q, Dong Q, Zhu W, Zhang X, Bu B, Wang W (2011) Glial gap junctional communication involvement in hippocampal damage after middle cerebral artery occlusion. *Ann Neurol* 70:121-132.
- Xu K, Moghal N, Egan SE (2012) Notch signaling in lung development and disease. *Adv Exp Med Biol* 727:89-98.
- Xu M, Zhang HL (2011) Death and survival of neuronal and astrocytic cells in ischemic brain injury: a role of autophagy. *Acta Pharmacol Sin* 32:1089-1099.
- Yoon K, Gaiano N (2005) Notch signaling in the mammalian central nervous system: insights from mouse mutants (vol 8, pg 709, 2005). *Nat Neurosci* 8:1411.
- Yu L, Li F, Zhao G, Yang Y, Jin Z, Zhai M, Yu W, Zhao L, Chen W, Duan W, Yu S (2015) Protective effect of berberine against myocardial ischemia reperfusion injury: role of Notch1/Hes1-PTEN/Akt signaling. *Apoptosis* 20:796-810.
- Zhang M, Wang C, Hu J, Lin J, Zhao Z, Shen M, Gao H, Li N, Liu M, Zheng P, Qiu C, Gao E, Wang H, Sun D (2015) Notch3/Akt signaling contributes to OSM-induced protection against cardiac ischemia/reperfusion injury. *Apoptosis* 20:1150-1163.
- Zhang X, Xu Y, Chen JM, Liu C, Du GL, Zhang H, Chen GF, Jiang SL, Liu CH, Mu YP, Liu P (2017) Huang Qi Decoction prevents BDL-induced liver fibrosis through inhibition of Notch signaling activation. *Am J Chin Med* 45:85-104.
- Zhao Z, Lu Z, Sun X, Zhao T, Zhang J, Zhou C, Zheng X, Zhang H, Shi G (2017) Global transcriptomic profiling of cortex and striatum: cerebral injury after ischemia/reperfusion in a mouse model. *J Stroke Cerebrovasc Dis* 26:1622-1634.
- Zhu J, Wang G, Yu Y, Yu Z, Xiao C, Wang Y (2012) Effects of transplantation with bone marrow-derived endothelial progenitor cells on learning, memory and neurons in the cortex of the parietal lobe after cerebral ischemia reperfusion injury of atherosclerotic model rats. *Jieyou Xuebao* 43:433-438.
- Zhu JD, Wang JJ, Ge G, Kang CS (2017) Effects of Noggin-transfected neural stem cells on neural functional recovery and underlying mechanism in rats with cerebral ischemia reperfusion injury. *J Stroke Cerebrovasc Dis* 26:1547-1559.